University of Crete

Mathematics and their Applications Master Program

MASTER THESIS on

Computational Methods on Atomistic and Quasi-Continuum Models

Virginia-Irene Kilikian

Supervisor : Prof Charalambos Makridakis

Heraklion, March 9, 2011

Committee members

Katsaounis Theodoros

Makridakis Charalambos

Rosakis Phoebus

Thanks - Acknowledgements

First of all, I would like to thank my supervisor, Charalambos Makridakis, for his essential help by offering a different perspective of mathematical modeling and suggesting to-the-point related bibliography and to Theodoros Katsaounis and Phoebus Rosakis for their time as members of my committee.

Also, I owe a big thanks to my family for providing for me for many years and through hard times without laying any pressure on me.

Last but not least, I dedicate this thesis to all my friends in the University of Crete who had to deal with my anxiety and nagging when things would not look good.

Summary

Continuum models are in most cases conditional approximations of atomistic models. Although the atomistic models are considered to capture in a more accurate way the true nature of significant applications, it is extremely difficult to base computational models on them, because of the vast number of unknowns due to the scale of the formulation. A kind of such atomistic models that is of interest are the crystal lattices models, which appear in modern material science. In a more macroscopic perspective, discrete models can be replaced by continuum ones described by PDEs, where difference operators are replaced by derivatives. However, it is already known that in many cases the continuum models fail to describe properly the behaviour of discrete equations. To tackle this fundamental issue, new methods are proposed : methods that picture the phenomena in a *quasi-continuum* way : in areas where the solution is expected to be relatively smooth, far from discontinuities and large gradients, the discrete lattice is replaced by a continuum material described by finite elements theory, while the initial discrete (atomistic) form is maintained in areas of non-smooth or large gradient solutions. The aim of this work is the study and analysis of methods with quasi-continuum approach in 1D.

Key words : quasicontinuum method, coupling, finite elements, coarse-graining, stresses, crystal deformation

Contents

1 Introduction

The idea of modeling an atomistic system without explicitly treating every atom of the domain is the baseline of all the methods presented in this project. This need comes naturally when simulating materials using a large amount of unknowns that make the fully atomistic representation too costly for a computational implementation. The problem of high computational cost of large-scale finite element analysis has been reported earlier [2]. On the other hand, coarse-graining may result in loss of important information. So, we try to significantly reduce the degrees of freedom (and, concequently, the energy calculations) and, at the same time, maintain atomistic detail wherever it is necessary. Systems that require atomistic scale information are, for instance, crack-tip studies, nano-identation, dislocation motion, the grain boundaries in certain applications and some tiny structures used in computer chips and micro-electronical systems. In such applications, it should be possible to treat the regions containing points of discontinuity with an atomistic point of view and use continuum mechanics to describe the behavior of the rest of the material.

The first method of this kind and the precursor of similar formulations was the *Quasicontinuum (QC) method*, developed by Tadmor, Ortiz and Phillips in 1996 [6]. They assumed that the exact description of the material at hand is the atomistic model and attempted to reproduce it with decreased computational cost. Given an interatomic potential (eg. Lennard-Jones, Morse) we look for equilibrium atomic configurations when external forces are applied. Recognizing that, even in the presence of defects, the bulk of the material will deform elastically and smoothly [5], the degrees of freedom are effectively reduced by defining a relatively small number of representative atoms (or *repatoms*) in areas where the deformation gradient changes gradually and approximating the positions of the atoms in-between through interpolation. At this point, it is important to highlight the fact that most continuous finite element techniques apply when the energy function is convex, which is not the case for atomistic models [5]. Also, equilibrium atomistic solutions are, in general, stable *local* minimizers of the energy functional, rather than *global* minimizers (however, in [18], there is a study of necessary conditions for global minimization).

To compute the total energy without having to compute every atom's separately, we apply the Cauchy-Born rule which states that all atoms in a uniformly deformed region contribute the same energy; therefore, for the calculation of the total energy we only need the repatoms (that form the finite elements) and *one* atom in each element. This is, roughly speaking, the formulation of the *local QC method*. Although the local QC succeeds in reducing the energy evaluations, it fails to represent accurately the energy of atoms on the interface of the finite elements and on the boundary of the

material.

Therefore, a *non-local* model is necessary. In practice, this involves computing the total energy or the forces (as the derivatives of the total energy) on each repatom and finding a configuration that minimizes the energy or is root of the forces. Apparently there are two approaches : the *energy-based* and the *force-based*. A fully non-local model has an increased computational cost compared to the local QC, so one wonders if he can benefit from both models without suffering from their drawbacks.

The real problem is how to couple the local and non-local models in one simulation. What is suggested is to divide the set of repatoms in two and use the local model for the one subset and the non-local model for the other. The result of this partition is the emergence of spurious forces, called *ghost forces* near the local - non-local interface that have no physical meaning. This was, by the way, the first energy-based method that was suggested. A means to overcome this difficulty is to add corrective forces near the interface (*Ghost Force Correction method, GFC* [12]) or use force-based formulation that doesn't derive from the differentiation of an energy functional.

The most popular force-based method and the starting point of a number of generalizations is the *QCF method*. The system is translated in terms of forces, (instead of energies) and typically there is also some coarse-graining in the region where the material deforms smoothly. Equilibrium can be sought as a configuration for which the force on each degree of freedom is zero either from explicit differentiation of an energy functional or directly from an approximate expression for the forces.

This thesis is divided into two Chapters : in Chapter 2, there is the mathematical formulation of the methods studied and the adopted notation. In Chapter 3, there is a presentation of the numerical results of the implementations in MATLAB.

2 Formulation of the methods

2.1 Problem setting in 1-D

The domain of the material in its reference state will be an infinite $2N$-periodic chain of equally-spaced atoms : the reference points are $\{x_i\}_{i\in\mathbb{Z}}$ and we look for deformations in the form of discrete functions $y_i = y(x_i)$ on the reference lattice with the property

$$y_{i+1+2N} - y_{i+2N} = y_{i+1} - y_i \qquad \forall i \in \mathbb{Z}$$

for a fixed $N \in \mathbb{N}$. We name the set of all such functions $\mathcal{A}_N$. From now on, we adopt the convention that all elements of $\mathcal{A}_N$ are identified with their continuous piecewise affine interpolants.

Step 1 We limit our study on intervals of length equal to the period $2N$, say the set $\mathcal{L} = \{-N+1,\cdots,N\}$. We also define the spacing constant $\varepsilon = 1/N$, the distance between two neighbouring atoms in an undeformed state. The nodes of $\mathcal{L}$ are illustrated below.

FIGURE 2.1: The reference cell $\mathcal{L} = \{-N+1,\cdots,N\}$.

Step 2 The next step is to divide the set of nodes $\mathcal{L}$ in two disjoint sets according to the accuracy we wish to achieve. For atoms in areas of smooth deformation we will use a coarse-grained continuum model and in non-smooth areas that present large variations we will keep the atomistic description (see Step 3). In the figure below, the white nodes are the ones in the continuum region and the black ones are in the atomistic region. We will often

also use the notation Ω_a and Ω_c for the atomistic and continuum domain respectively (more details in 2.3.3).

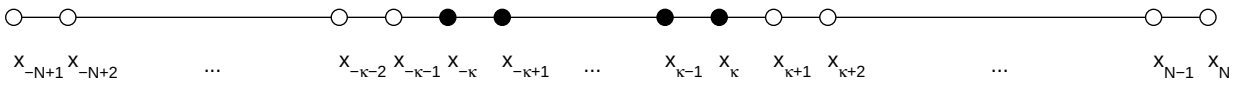

FIGURE 2.2: We separate the nodes in two distinct groups : where atomistic detail is required (black) and where a continuum description is adequate (white).

Step 3 The extra step that will significantly decrease the computational cost of our model is to coarsen the grid used in the continuum domain. This is feasible due to the assumption that the deformation of the material in hand is smooth in the particular area, so a P1 finite element approximation can be used for its description. This is done as follows : we define a subset $\mathcal{L} \supseteq \mathcal{L}_{rep} = \{i_1, \cdots, i_M\}$, the indexes of the so-called *repatoms*. Following the most commonly used setup, let's say that the "atomistic" region lies in $(x_{-\kappa}, x_\kappa)$ and the rest is the "continuum" region. In the set $\mathcal{L}_{rep}$ we will include all indexes $\mathcal{L}_a = \{-\kappa, \cdots, \kappa\}$ and name the rest of the nodes $\mathcal{L}_c = \mathcal{L}_{rep} \setminus \mathcal{L}_a$. . We name the reference positions of the repatoms X_i, $i = 1, \cdots, M$, so we end up with the following picture. Note that the spacing between the repatoms outside the atomistic region is not necessarily constant (later on, we will demand something more for $\mathcal{L}_c$, but for the time being this setup suffices). Of course, the repatoms are repeated periodically. Repatoms do not need to be on points of the atomic grid, as long as they satisfy a conservation of mass condition. This is useful for example to attempts of adaptive mesh, node distribution algorithms and automatic refinement [20, 2].

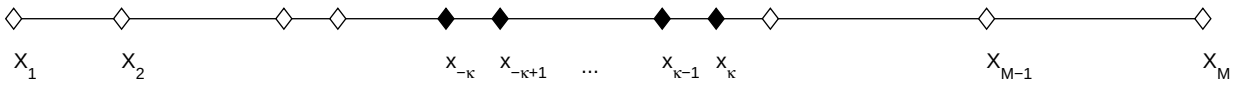

FIGURE 2.3: An example of a choice of repatoms.

2.2 The interatomic potential

The simulations contained in this work make use of a pair-wise description for atom interactions. The resulting energy can be considered in terms of two components: a long range interaction and a short range interaction. We assume that long range interactions are negligible and that short range interactions are approximated by pair potentials; atoms will interact according to a two-body potential ϕ (typically a Lennard-Jones or a Morse potential) in an up-to-R-neighbour style for a fixed $R \in \mathbb{N}$, i.e.

$$\phi : \mathbb{R}^+ \to \mathbb{R}$$
$$\phi(|y_i - y_j|) = 0, \text{ if } |i-j| > R$$

Some of the literature deals only with the case $R = 2$ [12, 14]. Our study doesn't make any assumptions about R.

Lennard-Jones potential The Lennard Jones potential (or 6-12 potential) is a mathematically simple model that approximates the interaction between a pair of neutral atoms or molecules. A form of the potential was first proposed in 1924 by John Lennard-Jones. Due to its simplicity it is the most popular potential function in molecular mechanics. In its general form the LJ potential is

$$\phi(r) = 4D_e \left\{ \left(\frac{\sigma}{r}\right)^{12} - \left(\frac{\sigma}{r}\right)^{6} \right\} \tag{2.1}$$

where D_e is the depth of the potential well and σ is the finite distance at which inter-particle potential is zero.

Morse potential The Morse potential is a convenient model for the potential energy of a diatomic molecule and can also be used to model other interactions, such as the interaction between an atom and a surface. It is of the form

$$\phi(r) = D_e(1 - \exp -\alpha(r - r_e))^2 \tag{2.2}$$

where D_e is again the depth of the potential well, r_e is the equilibrium bond distance and α controls the width of the well.

For the simulations, we used a LJ potential.

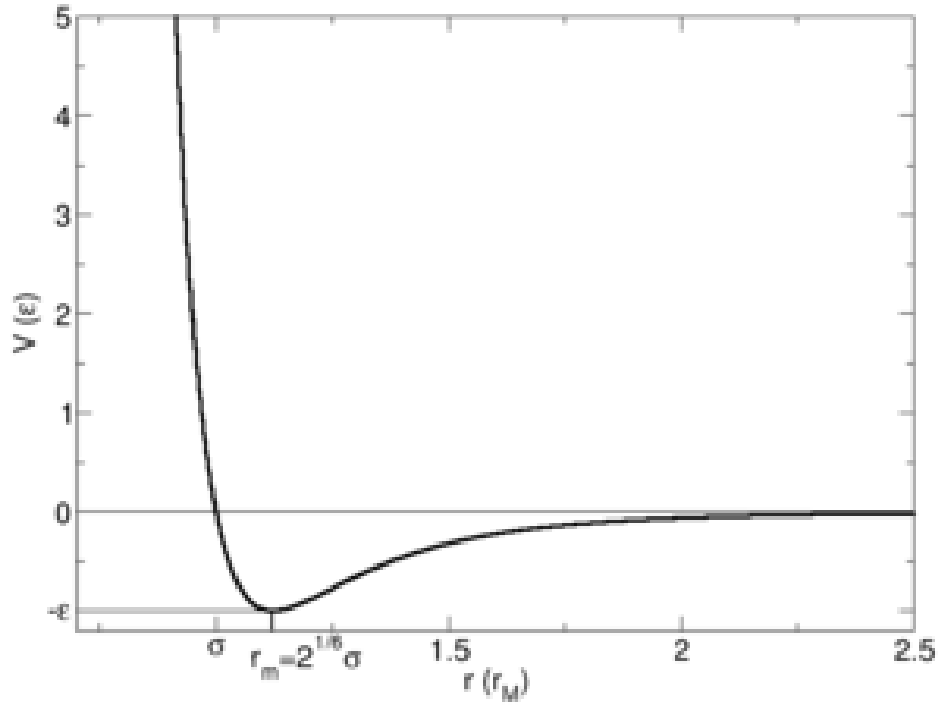

FIGURE 2.4: Lennard-Jones potential (source : wikimedia commons)

The values of the parameters of the definition (2.1) are selected based on the data of the problem (see also Chapter 3).

2.3 The Mathematical Models

2.3.1 Notation

For the setting presented in section 2.1 and a deformation $y \in \mathcal{A}_N$, we define the forward difference operators for all $r = 1, \cdots, R$

$$\begin{aligned} D_r &: y \to D_r y \\ (D_r y)_i &= \frac{y_{i+r} - y_i}{r\varepsilon} \end{aligned} \tag{2.3}$$

Note that D_r are linear, as for $\alpha \in \mathbb{R}$, $v \in \mathcal{A}_N$

$$\begin{aligned} (D_r(y+\alpha v))_i &= \frac{y_{i+r} + \alpha v_{i+r} - y_i - \alpha v_i}{r\varepsilon} \\ &= \frac{y_{i+r} - y_i}{r\varepsilon} + \alpha \frac{v_{i+r} - v_i}{r\varepsilon} \\ &= D_r y_i + \alpha D_r v_i \end{aligned}$$

We will also use the discrete derivative

$$y_i' = (D_1 y)_1 = \frac{y_{i+1} - y_i}{\varepsilon} \tag{2.4}$$

the norm on $\mathcal{A}_N$

$$\|y\|_{\mathcal{U}^{1,\infty}} = \max_{i \in \mathcal{L}} |y_i'| \tag{2.5}$$

and the inner product on $\mathcal{A}_N \times \mathcal{A}_N$

$$(v, w)_\varepsilon = \varepsilon \sum_{i \in \mathcal{L}} v_i w_i \tag{2.6}$$

2.3.2 The Atomistic Model (Step 1)

We will now introduce the basic atomistic model for the deformation of a 1-D crystal lattice, which is based on the principle that equilibrium states minimize the total energy. First, we define the space of admissible deformations, then

we write down an expression of the total energy of the system and then we compute the internal atomistic forces that will be used in the QCF model (Section 2.7). The deformation given by *this* model is considered to be the exact one and will be compared to other approximations.

We define the space of admissible deformations with the aid of the displacement space

$$\mathcal{U} = \left\{ v \in \mathcal{A}_N : \left(v, \widetilde{1} \right)_\varepsilon = 0 \right\} \tag{2.7}$$

where $\widetilde{1} = (1)_{i\in\mathbb{Z}}$. For a constant uniform deformation B, we define the set of deformations as

$$\mathcal{Y}^+ = \left\{ y \in Bx + \mathcal{U} : y_i' > 0 \quad \forall i \in \mathbb{Z} \right\} \tag{2.8}$$

So, we focus on periodic deformations with zero mean displacement from the homogeneous lattice Bx with positive discrete derivatives[1].

If the two-body potential ϕ is known (in our case, LJ potential (2.1)), then the internal atomic energy for a displacement $y \in \mathcal{Y}^+$ is given by

$$E^a(y) = \varepsilon \sum_{r=1}^{R} \sum_{i\in\mathcal{L}} \phi(rD_r y_i) \tag{2.9}$$

Its variation (or more precisely, its Fréchet derivative) is the bounded linear operator

$$\begin{aligned} DE^a(y) &: \mathcal{U} \to \mathbb{R} \\ DE^a(y;v) &= \varepsilon \sum_{r=1}^{R} \sum_{i\in\mathcal{L}} \phi'(rD_r y_i) \cdot rD_r v_i \end{aligned} \tag{2.10}$$

Proof of (2.10).

$$E^a(y) = \varepsilon \sum_{r=1}^{R} \sum_{i\in\mathcal{L}} E^a_{r,i}(y) \tag{2.11}$$

where

$$\begin{aligned} E^a_{r,i} &: \mathcal{Y}^+ \to \mathbb{R} \\ E^a_{r,i}(y) &= \phi(rD_r y_i) \end{aligned} \tag{2.12}$$

so, due to linearity in (2.11), $E^a(y)$ is Fréchet differentiable, if all $E^a_{r,i}(y)$ are Fréchet differentiable and

[1] The reason for this restriction is that potential functions give arbitrarily high values for $r \to 0$. As there is no physically correct way to cross the origin in a continuous manner, we will only use positive differences $y_{i+r} - y_i$.

$$DE^a(y;v) = \sum_{r=1}^{R} \sum_{i \in \mathcal{L}} DE^a_{r,i}(y;v) \tag{2.13}$$

First we compute the Gâteaux derivatives $DE^a_{r,i}(y;v)$:

$$\begin{aligned}
DE^a_{r,i}(y;v) &= \lim_{\tau \to 0} \frac{E^a_{r,i}(y+\tau v) - E^a_{r,i}(y)}{\tau} \\
&= \frac{d}{d\tau} E^a_{r,i}(y+\tau v)|_{\tau=0} \\
&= \frac{d}{d\tau} \phi\left(r\left(D_r(y+\tau v)\right)_i\right)|_{\tau=0} \\
&= \frac{d}{d\tau} \phi\left(rD_r y_i + r\tau D_r v_i\right)|_{\tau=0} \\
&= \phi'\left(rD_r y_i + r\tau D_r v_i\right) \cdot rD_r v_i|_{\tau=0} \\
&= \phi'(rD_r y_i) \cdot rD_r v_i
\end{aligned}$$

Now, to verify that $DE^a_{r,i}$ are also the Fréchet derivatives, we check if the following limits exist and

$$\lim_{v \to 0} \frac{\left|E^a_{r,i}(y+v) - E^a_{r,i}(y) - DE^a_{r,i}(y;v)\right|}{\|v\|_{\mathcal{U}^{1,\infty}}} = 0, \quad \forall i \in \mathcal{L},\, r = 1, \cdots, R$$

$$\begin{aligned}
&\frac{\left|E^a_{r,i}(y+v) - E^a_{r,i}(y) - DE^a_{r,i}(y;v)\right|}{\|v\|_{\mathcal{U}^{1,\infty}}} = \\
&= \frac{\left|\phi(r\varepsilon D_r y_i + r\varepsilon D_r v_i) - \phi(r\varepsilon D_r y_i) - \phi'(r\varepsilon D_r y_i) \cdot r\varepsilon D_r v_i\right|}{\|v\|_{\mathcal{U}^{1,\infty}}} \\
&= \frac{\left|\frac{1}{2}\phi''(r\varepsilon D_r y_i) \cdot (r\varepsilon D_r v_i)^2 + O\left[(r\varepsilon D_r v_i)^3\right]\right|}{\|v\|_{\mathcal{U}^{1,\infty}}} \\
&\leq \frac{\left|\frac{1}{2}\phi''(r\varepsilon D_r y_i) \cdot r^2 \|v\|^2_{\mathcal{U}^{1,\infty}} + O\left(\|v\|^3_{\mathcal{U}^{1,\infty}}\right)\right|}{\|v\|_{\mathcal{U}^{1,\infty}}} \xrightarrow{v \to 0} 0
\end{aligned}$$

■

Next, we perform the *patch test* which indicates if the method is consistent.

The patch test : to ensure convergence of a method that approximates total energy by a function $\widetilde{E}(y)$ it must be true that for the uniform deformation $y = Bx$

$$D\widetilde{E}(Bx;v) = 0 \quad \forall v \in \mathcal{U} \tag{2.14}$$

Indeed,

$$\begin{aligned} DE^a(Bx;v) &= \varepsilon \sum_{r=1}^{R} \sum_{i\in\mathcal{L}} \phi'(rB)\cdot rD_r v_i \\ &= \sum_{r=1}^{R} \left[r\phi'(rB) \sum_{i\in\mathcal{L}} (v_{i+r} - v_i) \right] = 0 \quad \forall v \in \mathcal{U} \end{aligned} \tag{2.15}$$

due to periodicity of v. In general, to include external forces, we introduce $g \in \mathcal{U}$ a vector with dead loads on the nodes and hence the total energy will be

$$E^a_{tot}(y) = E^a(y) - (g,y)_\varepsilon \tag{2.16}$$

and we seek a local minimizer

$$y^a \in \mathcal{Y}^+ : E^a_{tot}(y^a) = \min_{y\in\mathcal{Y}^+} E^a_{tot}(y) \tag{2.17}$$

It is easy to prove that the variation of E^a_{tot} is

$$DE^a_{tot}(y;v) = \varepsilon \sum_{r=1}^{R} \sum_{i\in\mathcal{L}} \phi'(rD_r y_i)\cdot rD_r v_i - \varepsilon \sum_{i\in\mathcal{L}} g_i v_i \tag{2.18}$$

A necessary condition for $y^a \in \mathcal{Y}^+$ to be a solution to (2.17) is to satisfy the condition

$$DE^a_{tot}(y^a;v) = 0 \quad \forall v \in \mathcal{U} \tag{2.19}$$

If we collect the internal atomistic forces in a vector $f^a(y)$, where

$$f^a_i(y) = -\frac{1}{\varepsilon}\frac{\partial E^a(y)}{\partial y_i} \quad \forall i \in \mathbb{Z} \tag{2.20}$$

we can rewrite the condition (2.19), in the equivalent form

$$(f^a(y^a) + g, v)_\varepsilon = 0 \qquad \forall v \in \mathcal{U} \tag{2.21}$$

Proof that (2.19) $\Rightarrow$ (2.21). First, note that

$$\begin{aligned}\frac{\partial E^a(y^a)}{\partial y_i} &= \varepsilon \sum_{r=1}^{R} \left[\frac{\partial}{\partial y_i} \sum_{j=-N+1}^{N} \phi\left(\frac{y^a_{j+r} - y^a_j}{\varepsilon} \right) \right] \\ &= \sum_{r=1}^{R} \left[\phi'\left(\frac{y^a_i - y^a_{i-r}}{\varepsilon} \right) - \phi'\left(\frac{y^a_{i+r} - y^a_i}{\varepsilon} \right) \right] \end{aligned} \tag{2.22}$$

Now, suppose $y^a \in \mathcal{Y}^+$ satisfies (2.19) and $v \in \mathcal{U}$. Then,

$$\begin{aligned}(f^a(y^a) + g, v)_\varepsilon &= (f^a(y^a), v)_\varepsilon + (g, v)_\varepsilon \\ &= -\sum_{i=-N+1}^{N} \frac{\partial E^a(y^a)}{\partial y_i} \cdot v_i + \varepsilon \sum_{i=-N+1}^{N} g_i v_i \\ &\overset{(2.19)}{=} -\sum_{i=-N+1}^{N} \frac{\partial E^a(y^a)}{\partial y_i} \cdot v_i + \varepsilon \sum_{r=1}^{R} \sum_{i \in \mathcal{L}} \phi'(r D_r y^a_i) \cdot r D_r v_i \\ &= -\sum_{i=-N+1}^{N} \frac{\partial E^a(y^a)}{\partial y_i} \cdot v_i + \sum_{r=1}^{R} \sum_{i \in \mathcal{L}} \phi'\left(\frac{y^a_{i+r} - y^a_i}{\varepsilon} \right) \cdot (v_{i+r} - v_i) \\ &= \sum_{i=-N+1}^{N} \left[-\frac{\partial E^a(y^a)}{\partial y_i} \cdot v_i + \sum_{r=1}^{R} \phi'\left(\frac{y^a_{i+r} - y^a_i}{\varepsilon} \right) \cdot (v_{i+r} - v_i) \right] \\ &\overset{(2.22)}{=} \sum_{i=-N+1}^{N} \left[v_i \cdot \sum_{r=1}^{R} \phi'\left(\frac{y^a_{i+r} - y^a_i}{\varepsilon} \right) - v_i \cdot \sum_{r=1}^{R} \phi'\left(\frac{y^a_i - y^a_{i-r}}{\varepsilon} \right) + \right. \\ &\qquad \left. + \sum_{r=1}^{R} v_{i+r} \cdot \phi'\left(\frac{y^a_{i+r} - y^a_i}{\varepsilon} \right) - v_i \cdot \sum_{r=1}^{R} \phi'\left(\frac{y^a_{i+r} - y^a_i}{\varepsilon} \right) \right] \\ &= \sum_{i \in \mathcal{L}} \sum_{r=1}^{R} \left[v_{i+r} \cdot \phi'\left(\frac{y^a_{i+r} - y^a_i}{\varepsilon} \right) - v_i \cdot \phi'\left(\frac{y^a_i - y^a_{i-r}}{\varepsilon} \right) \right] \\ &= \sum_{r=1}^{R} \left[\sum_{i=-N+1}^{N} v_{i+r} \cdot \phi'\left(\frac{y^a_{i+r} - y^a_i}{\varepsilon} \right) - \sum_{i=-N+1}^{N} v_i \cdot \phi'\left(\frac{y^a_i - y^a_{i-r}}{\varepsilon} \right) \right] \\ &= \sum_{r=1}^{R} \left[\sum_{i=-N+1}^{N} v_{i+r} \cdot \phi'\left(\frac{y^a_{i+r} - y^a_i}{\varepsilon} \right) - \sum_{i=-N+1-r}^{N-r} v_{i+r} \cdot \phi'\left(\frac{y^a_{i+r} - y^a_i}{\varepsilon} \right) \right] \\ &= 0 \qquad \text{due to periodicity of functions } v, y \end{aligned}$$

■

The formula (2.21) is the strong formulation of the atomistic model.

2.3.3 The Continuum Model (Step 2)

In a region Ω_c where the deformation is smooth, instead of the atomistic model we can use a continuum one. The most commonly used continuum model is the Cauchy-Born approximation, which results in

$$E^c(y) = \sum_{r=1}^{R} \int_{\Omega_c} \phi(ry'(x))dx \tag{2.23}$$

where $y \in W^{1,\infty}$ is the continuum approximation of the discrete function y_i we used so far and y' is its weak derivative. A way to see how (2.23) works is to use the energy density

$$W(\alpha) = \sum_{r=1}^{R} \phi(r\alpha) \tag{2.24}$$

and identify the energy as

$$E^c(y) = \int_{\Omega_c} W(y'(x))dx \tag{2.25}$$

Just as we did for the atomistic formulation, we write down the variation of $E^c(y)$, $y \in \mathcal{Y}^+$ as

$$\begin{aligned} DE^c(y) &: \mathcal{U} \to \mathbb{R} \\ DE^c(y;v) &= \sum_{r=1}^{R} \int_{\Omega_c} \phi'(ry'(x)) \cdot rv'(x)dx \end{aligned} \tag{2.26}$$

Proof of (2.26). Write

$$E^c(y) = \sum_{r=1}^{R} E_r^c(y)$$

where

$$\begin{aligned} E_r^c &: \mathcal{Y}^+ \to \mathbb{R} \\ E_r^c(y) &= \int_{\Omega_c} \phi(ry'(x))dx \end{aligned} \tag{2.27}$$

The Gâteaux derivatives are

$$\begin{aligned} DE_r^c(y;v) &= \frac{d}{d\tau}E_r^c(y+\tau v)|_{\tau=0} \\ &= \frac{d}{d\tau}\int_{\Omega_c}\phi(ry'(x)+r\tau v'(x))dx|_{\tau=0} \\ &= \int_{\Omega_c}\frac{d}{d\tau}\phi(ry'(x)+r\tau v'(x))dx|_{\tau=0} \\ &= \int_{\Omega_c}\phi'(ry'(x)+r\tau v'(x))\cdot rv'(x)dx|_{\tau=0} \\ &= \int_{\Omega_c}\phi'(ry'(x))\cdot rv'(x)dx \end{aligned}$$

so it's left to verify that

$$\frac{|E_r^c(y+v)-E_r^c(y)-DE_r^c(y;v)|}{\|v\|_{\mathcal{U}^{1\infty}}} \xrightarrow{v\to 0} 0 \tag{2.28}$$

$$\begin{aligned} \frac{|E_r^c(y+v)-E_r^c(y)-DE_r^c(y;v)|}{\|v\|_{\mathcal{U}^{1\infty}}} &= \frac{\left|\int_{\Omega_c}\phi(ry'(x)+rv'(x))-\phi(ry'(x))-\phi'(ry'(x))\cdot rv'(x)dx\right|}{\|v\|_{\mathcal{U}^{1,\infty}}} \\ &\le \frac{\int_{\Omega_c}\left|\frac{1}{2}r^2(v'(x))^2\cdot\phi''(ry'(x))+O\left[(v'(x))^3\right]\right|dx}{\|v\|_{\mathcal{U}^{1,\infty}}} \\ &\le \frac{r^2\|v\|_{\mathcal{U}^{1,\infty}}^2\int_{\Omega_c}\left|\phi''(ry'(x))\right|dx+O(\|v\|_{\mathcal{U}^{1,\infty}}^3)}{\|v\|_{\mathcal{U}^{1,\infty}}} \xrightarrow{v\to 0} 0 \end{aligned}$$

So

$$DE_r^c(y;v) = \int_{\Omega_c}\phi'(ry'(x))\cdot rv'(x)dx \tag{2.29}$$

Consequently,

$$DE^c(y;v) = \sum_{r=1}^{R}\int_{\Omega_c}\phi'(ry'(x))\cdot rv'(x)dx \tag{2.30}$$

■

The total energy for a deformation $y\in\mathcal{Y}^+$ is

$$E_{tot}^c(y) = E^c(y)-(g,y)_\varepsilon \tag{2.31}$$

2.3.4 The Coarse-grained Model (Step 3) - Local QC (QCL)

As we briefly described in Section 2.1, in order to limit the computational cost in regions where it is not necessary to be very scholastic, we define the set of repatoms in one period

$$\mathcal{L}_{rep} = \{i_1, \cdots, i_M\} \subseteq \mathcal{L} \tag{2.32}$$

and to be consistent we extend it $2N$-periodically :

$$i_{m+M} = i_m + 2N \quad \forall m \in \mathbb{Z}$$

Then we are able to define the reference positions of repatoms $X_m = x_{i_m}$, the mesh size for elements $h_m = X_m - X_{m-1}$ and the mesh size for nodes $H_m = \frac{1}{2}(X_{m+1} - X_{m-1})$. We are now ready to define the spaces of the coarse-grained solutions; the intermediate step of the continuum model will not be present in the final formulation. Only the coarse-grained version will be used from now on. We begin with the set $\mathcal{T}_h^1$, the space of piecewise linear functions with respect to the new mesh $(X_m)_{m\in\mathbb{Z}}$. Every $u_h \in \mathcal{T}_h^1$ is uniquely determined by its nodal values $U_m = u_h(X_m) = u_{h,i_m}$ and, after observing that its gradient in the interval (X_{m-1}, X_m) is exactly equal to $U'_m = \frac{U_m - U_{m-1}}{h_m}$, then the values of the nodes with indexes between i_{m-1} and i_m are

$$u_h(x_i) = u_{h,i} = U_{m-1} + U'_m(x_i - X_{m-1}), \quad i = i_{m-1}, \cdots, i_m \tag{2.33}$$

Proof of (2.33). By definition of $\mathcal{T}_h^1$, u_h is a linear function on every interval of the form (X_{m-1}, X_m).

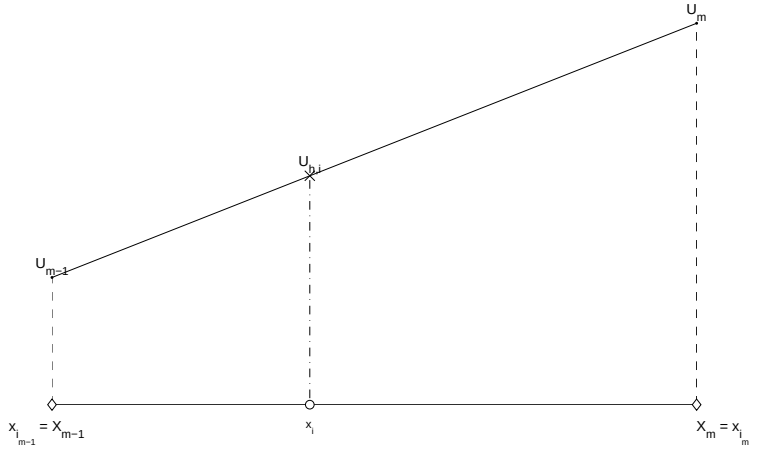

$$\left.\begin{array}{rcl} u_h|_{[X_{m-1},X_m]} &=& \alpha x + \beta \\ u_h(X_{m-1}) &=& U_{m-1} \\ u_h(X_m) &=& U_m \end{array}\right\} \Rightarrow u_h|_{[X_{m-1},X_m]} = U_{m-1} + U'_m(x - X_{m-1}) \overset{x=x_i}{\Rightarrow}$$

$$u_{h,i} = U_{m-1} + U'_m(x_i - X_{m-1})$$

■

For the time being, assume $\mathcal{L}_{rep} = \mathcal{L}$ (in other words $\Omega_c = (x_{-N+1}, x_N)$). The spaces of functions we use in this coarse-grained version are based on the inner product

$$(v,w)_h = \sum_{m=1}^{M} H_m v_{i_m} w_{i_m} \tag{2.34}$$

which is defined for two discrete functions $v, w \in \mathcal{A}_N$; actually, v and w only need to be defined on the set $\mathcal{L}_{rep}$. The inner product (2.34) is an approximation of the ε-inner product (2.6) used in the atomistic (exact) model and will be used in the same way. The displacement space and deformation space are then defined in a way similar to the atomistic ones

$$\mathcal{U}_h = \left\{ v_h \in \mathcal{A}_N \cap \mathcal{T}_h^1 \,:\, \left(v, \widetilde{1}\right)_h = 0 \right\} \tag{2.35}$$

$$\mathcal{Y}_h^+ = \left\{ y_h \in \mathcal{Y}_h \,:\, y'_{h,i} > 0 \quad \forall i \in \mathbb{Z} \right\} \tag{2.36}$$

The energy of a deformation $y_h \in \mathcal{Y}_h^+$ is an approximation to E_{tot}^c (2.25) and is given by

$$E^{c,h}(y_h) = \sum_{m=1}^{M} h_m W(Y'_m) \tag{2.37}$$

If we collect the nodal values of y_h and external forces g with respect to the mesh (X_m) in $Y \in \mathbb{R}^M$ and $G \in \mathbb{R}^M$ respectively, the total continuum energy $E_{tot}^{c,h}$ is given by

$$E_{tot}^{c,h}(y_h) = E^{c,h}(y_h) - (G,Y)_h \tag{2.38}$$

and the problem is reduced to finding a local minimizer

$$y_h \in \mathcal{Y}_h^+ \,:\, E_{tot}^{c,h}(y_h) = \min_{y \in \mathcal{Y}_h^+} E_{tot}^{c,h}(y) \tag{2.39}$$

A necessary condition for $y_h \in \mathcal{Y}_h^+$ to be a solution to (2.39) is to satisfy

$$DE_{tot}^{c,h}(y_h; v_h) = 0 \qquad \forall v_h \in \mathcal{U}_h \tag{2.40}$$

The analogue of the internal atomic forces $f^a(y)$ defined in the atomistic model are the generalized forces F^c

$$F^c_m(y_h) = -\frac{1}{H_m}\frac{\partial E^{c,h}(y_h)}{\partial Y_m} \qquad \forall m \in \mathbb{Z} \tag{2.41}$$

so we get the condition

$$(F^c(y_h) + g, v_h)_h = 0 \qquad \forall v_h \in \mathcal{U}_h \tag{2.42}$$

which is equivalent to the condition (2.40).

Proof of (2.40) $\Rightarrow$ (2.42). First, note that

$$\begin{aligned}\frac{\partial E^{c,h}(y_h)}{\partial Y_i} &= \frac{\partial}{\partial Y_i}\sum_{m=1}^{M} h_m W\left(\frac{Y_m - Y_{m-1}}{h_m}\right) \\ &= W'\left(\frac{Y_i - Y_{i-1}}{h_i}\right) - W'\left(\frac{Y_{i+1} - Y_i}{h_{i+1}}\right)\end{aligned} \tag{2.43}$$

Now, suppose $y_h \in \mathcal{Y}_h^+$ satisfies (2.40) and $v_h \in \mathcal{U}_h$. Then,

$$(2.40) \Rightarrow \sum_{m=1}^{M} h_m W'(Y'_m)\cdot V'_m - \sum_{m=1}^{M} H_m g_{i_m} V_m = 0 \tag{2.44}$$

$$\Rightarrow \sum_{m=1}^{M} W'(Y'_m)\cdot(V_m - V_{m-1}) - (g, v_h)_h = 0 \tag{2.45}$$

and

$$
\begin{aligned}
(F^c(y_h)+g,v_h)_h &= (F^c(y_h),v_h)_h + (g,v_h)_h \\
&\overset{(2.45)}{=} -\sum_{m=1}^{M} \frac{\partial E^{c,h}(y_h)}{\partial Y_m}\cdot V_m + \sum_{m=1}^{M} W'(Y'_m)\cdot(V_m - Vm-1) \\
&\overset{(2.43)}{=} \sum_{m=1}^{M}\left[-W'\left(\frac{Y_m-Y_{m-1}}{h_m}\right)\cdot V_m + W'\left(\frac{Y_{m+1}-Y_m}{h_{m+1}}\right)\cdot V_m + \right. \\
&\qquad \left. + W'\left(\frac{Y_m-Y_{m-1}}{h_m}\right)\cdot(V_m - V_{m-1})\right] \\
&= \sum_{m=1}^{M}\left[V_m\cdot W'\left(\frac{Y_{m+1}-Y_m}{h_{m+1}}\right) - V_{m-1}\cdot W'\left(\frac{Y_m-Y_{m-1}}{h_m}\right)\right] \\
&= \sum_{m=1}^{M}\sum_{r=1}^{R}\left[rV_m\cdot\phi'\left(r\frac{Y_{m+1}-Y_m}{h_{m+1}}\right) - rV_{m-1}\cdot\phi'\left(r\frac{Y_m-Y_{m-1}}{h_m}\right)\right] \\
&= \sum_{r=1}^{R} r\left[\sum_{m=1}^{M} V_m\cdot\phi'\left(r\frac{Y_{m+1}-Y_m}{h_{m+1}}\right) - \sum_{m=1}^{M} V_{m-1}\cdot\phi'\left(r\frac{Y_m-Y_{m-1}}{h_m}\right)\right] \\
&= \sum_{r=1}^{R} r\left[\sum_{m=1}^{M} V_m\cdot\phi'\left(r\frac{Y_{m+1}-Y_m}{h_{m+1}}\right) - \sum_{m=0}^{M-1} V_m\cdot\phi'\left(r\frac{Y_{m+1}-Y_m}{h_{m+1}}\right)\right] \\
&= 0 \qquad \text{due to periodicity of } v_h, y_h
\end{aligned}
$$

■

The criticality condition (2.42) is the strong formulation of the QCL method (Quasi Continuum Local), which keeps a continuum approach in the whole domain. Apparently, this will not be enough if the material in hand presents cracks and steep dislocations.

2.4 The QCE method - the emergence of ghost forces

Having defined all the forces and criticality conditions, what is left is to decide how to use them according to the specific setting in 1-D we have described earlier. The essence of the QC notion is how to couple the two formulations in one method and what happens across the interface between the atomistic and the continuum regions. From now on we will demand that the choice of repatoms is such that $\{-\kappa-R,\cdots,\kappa+R\}\subseteq\mathcal{L}_{rep}$. So far, we have introduced two modes of numbering atoms : the purely atomistic one with indexes in $\mathcal{L}$ and the one using repatoms with indexes in $\{1,\cdots,M\}$ and, as mentioned earlier, they are related by the sequence $i_m : X_m = x_{i_m}$. This relation is not very easy to handle; from now on, to use a common symbolism, we will use the symbols $L,U\in\{1,\cdots,M\}$ to denote the repatoms on the interface, meaning

$$i_L = -\kappa, \qquad i_U = \kappa \tag{2.46}$$

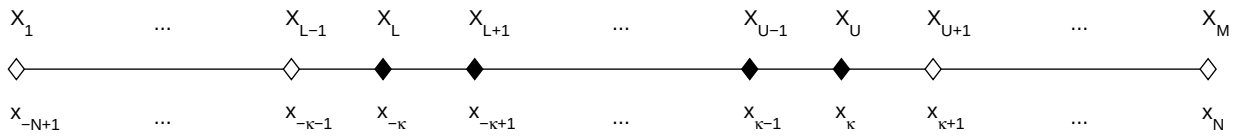

FIGURE 2.5: The two styles of enumerating the atoms. The top row contains the repatoms and the bottom row the original atoms.

The first energy-based model, the QCE method [6], attempted a straightforward coupling : write down the atomistic (exact) energy for a $y_h \in \mathcal{Y}_h^+$ as

$$\begin{aligned} E^a(y) &= \sum_{i=-N+1}^{N} \sum_{r=1}^{R} \varepsilon\phi(rD_r y_i) \\ &\approx \sum_{m=L}^{U} \sum_{r=1}^{R} \varepsilon\phi\left(r\left(D_r y_h\right)_{i_m}\right) + \sum_{m=1}^{L-1} h_m W(Y_m') + \sum_{m=U+1}^{M} h_m W(Y_m') = E^{qce}(y_h) \end{aligned} \tag{2.47}$$

So, the atoms $x_{-\kappa}, \cdots, x_\kappa$ are treated atomistically, whereas the rest use the form of the continuum energy $E^{c,h}$.

$$\begin{aligned} DE^{qce}(y_h; v_h) = &\sum_{m=L}^{U} \sum_{r=1}^{R} \varepsilon\phi'\left(r\left(D_r y_h\right)_{i_m}\right) \cdot r\left(D_r v_h\right)_{i_m} + \\ &+ \sum_{m=1}^{L-1} \sum_{r=1}^{R} h_m r\phi'(rY_m') \cdot V_m' + \sum_{m=U+1}^{M} \sum_{r=1}^{R} h_m r\phi'(rY_m') \cdot V_m' \end{aligned}$$

Applying the patch test (2.14) for the nearest neighbor interaction ($R = 1$), we have:

$$\begin{aligned} DE^{qce}(Bx; v_h) = &\phi'(B) \cdot \left[\sum_{m=L}^{U} (v_{h,i_m+1} - v_{h,i_m}) + \right. \\ &\left. + \sum_{m=1}^{L-1} (V_m - V_{m-1}) + \sum_{m=U+1}^{M} (V_m - V_{m-1}) \right] \end{aligned}$$

$$= \phi'(B) \cdot [(V_{U+1} - V_L) + (V_{L-1} - V_0) + (V_M - V_U)]$$

$$\overset{V_0 = V_M}{=} \phi'(B) \cdot [V_{U+1} - V_L + V_{L-1} - V_U]$$

This is not necessarily zero for every $v_h \in \mathcal{U}_h$. The terms that bother us arise around the interface and they are known

in the field as *ghost forces*, as they have no physical meaning. The problem of ghost forces emerges for most energy-based methods, reducing their accuracy due to interfacial errors, but a lot of effort has been made to go around it. Some techniques are GFC(Ghost Force Correction) (see [12, 13, 15, 16, 17]), coupling of length scales, GCS(Geometrically Consistent Scheme) etc. The reason seems to be that we use energy contribution per atom, missing some information when we switch from atomistic to continuum approach. More specifically, there is an asymmetry, as a repatom X_α in Ω_a will not be affected by a repatom X_β in Ω_c near the interface, but X_β, that interacts according to the continuum model, will be affected by the displacement of X_α (see also [20]). This is not the case for the force-based methods, where a similar methodology doesn't lead to errors on the interface.

2.5 The ECC Method

This method, as well as the next one, was proposed by A.Shapeev in [1]. It is based on the concept of dividing the contributions to the total energy (2.9) of bonds in two : the exact ones and the continuum ones. For a more understandable presentation, we begin with no coarsening. In the atomistic system, we define the set of all bonds as all the possible open intervals with up-to-R-neighbouring atoms as end points. Formally,

$$\mathcal{B} := \{(x_i, x_{i+r}),\, 1 \le r \le R,\, i \in \mathcal{L}\} \tag{2.48}$$

The idea is to write down the atomistic energy (2.9) in terms of an exact contribution of all bonds in $\mathcal{B}$. This is achieved by simply defining for any $(x_i, x_{i+r}) = b_{i,r}$ (or simply b) $\in \mathcal{B}$ its exact contribution as

$$e_b(y) = \varepsilon\phi(rD_r y_i) \tag{2.49}$$

and it is clear that

$$E^a(y) = \sum_{b\in\mathcal{B}} e_b(y) \tag{2.50}$$

The trick is to treat the bonds lying entirely inside the continuum area Ω_c in a different way using their continuum contribution

$$c_b(y) = \frac{1}{r}\int_{x_i}^{x_{i+r}} \phi(ry'(x))dx \tag{2.51}$$

This is allowed, because these two contributions have the same variation for a uniform deformation $y = Bx$:

$$
\begin{aligned}
e_b(y) &= \varepsilon\phi(rD_r y_i) \\
\Rightarrow De_b(y;v) &= \varepsilon\phi'(rD_r y_i)\cdot rD_r v_i \\
\overset{y=Bx}{\Rightarrow} De_b(Bx;v) &= \phi'(rB)\cdot(v_{i+r}-v_i)
\end{aligned}
\tag{2.52}
$$

$$
\begin{aligned}
c_b(y) &= \frac{1}{r}\int_{x_i}^{x_{i+r}} \phi(ry'(x))dx \\
\Rightarrow Dc_b(y;v) &= \frac{1}{\cancel{r}}\int_{x_i}^{x_{i+r}} \phi'(ry'(x))\cdot \cancel{r}v'(x)dx \\
\overset{y=Bx}{\Rightarrow} Dc_b(Bx;v) &= \phi'(rB)\cdot(v_{i+r}-v_i)
\end{aligned}
$$

So the atomistic energy (2.9) is approximated by

$$
E^a(y) \approx E^{ecc}(y) := \sum_{\substack{b\in\mathcal{B}\\ b\not\subset\Omega_c}} e_b(y) + \sum_{\substack{b\in\mathcal{B}\\ b\subset\Omega_c}} c_b(y) \tag{2.53}
$$

2.6 The ACC Method

The previous method actually treated all bonds located entirely inside the continuum region with a continuum approximation and all other bonds used atomistic approximations. The concept of this method is based on the bonds we defined earlier but this time every bond has *both* an atomistic and a continuum contribution to the total energy. The setting we are working on will simplify some definitions we will need. Recall that the atomistic region is $\Omega_a = (x_{-\kappa}, x_\kappa)$; for a bond $b = (x_i, x_{i+r})$ we will use the following symbols : the open interval $b \cap \Omega_a$ will be (l_b, r_b) and the remaining endpoint will be c_b. The following figure shows the possible relative positions of Ω_a and an intersecting bond $\mathcal{B} \ni b = (x_i, x_{i+r})$.

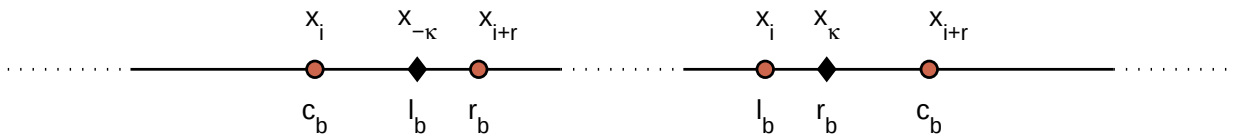

FIGURE 2.6: The continuum region is marked with a black line and the atomistic with a white line. The interface points are black and the endpoints of b are colored purple.

Lastly, we will need the definition of a generalization of the discrete forward difference operator we have used so far.

For an open interval $\omega = (l_\omega, r_\omega)$, we define

$$\begin{aligned} D_\omega &: y \to D_\omega y \\ D_\omega y &= \frac{1}{|\omega|}\left(y(r_\omega) - y(l_\omega)\right) \end{aligned} \tag{2.54}$$

Our purpose is to use a proportion of the atomistic contribution we defined earlier; this proportion is determined by the measure of $b \cap \Omega_a$ compared to the overall measure of b itself. A similar strategy is used for the continuum part. Put in formulas, the atomistic contribution is

$$a_b(y) := \frac{|b \cap \Omega_a|}{r\varepsilon}\phi(rD_{b\cap\Omega_a} y) \tag{2.55}$$

and the continuum contribution is

$$c_b(y) := \frac{1}{r\varepsilon}\int_{b\cap\Omega_c} \phi(ry'(x))dx \tag{2.56}$$

For a uniform deformation $y = Bx$ we compute the variation of a_b and c_b:

$$\begin{aligned} a_b(y) &= \frac{|b \cap \Omega_a|}{r\varepsilon}\phi\left(rD_{b\cap\Omega_a} y\right) \\ \Rightarrow Da_b(y;v) &= \frac{|b \cap \Omega_a|}{\cancel{r}\varepsilon}\phi'(rD_{b\cap\Omega_a} y)\cdot \cancel{r} D_{b\cap\Omega_a} v \\ \overset{y=Bx}{\Rightarrow} Da_b(Bx;v) &= \frac{|b \cap \Omega_a|}{\varepsilon}\phi'(rB)\cdot(v(r_b) - v(l_b)) \end{aligned}$$

$$\begin{aligned} c_b(y) &= \frac{1}{r\varepsilon}\int_{b\cap\Omega_c} \phi(ry'(x))dx \\ \Rightarrow Dc_b(y;v) &= \frac{1}{\cancel{r}\varepsilon}\int_{b\cap\Omega_c} \phi'(ry'(x))\cdot \cancel{r} v'(x)dx \\ \overset{y=Bx}{\Rightarrow} Dc_b(Bx;v) &= \frac{|b \cap \Omega_c|}{\varepsilon}\phi'(rB)\cdot(v(r_b) - v(l_b)) \end{aligned}$$

and the sum

$$
\begin{aligned}
Da_b(Bx;v) + Dc_b(Bx;v) &= \frac{|b\cap\Omega_a|}{\varepsilon}\phi'(rB)\cdot D_{b\cap\Omega_a}v + \frac{|b\cap\Omega_c|}{\varepsilon}\phi'(rB)\cdot D_{b\cap\Omega_c}v \\
&= \frac{1}{\varepsilon}\phi'(rB)\cdot(v_{i+r}-v_i) \\
&\overset{(2.52)}{=} \frac{1}{\varepsilon}\cdot De_b(Bx;v) \qquad (2.57)
\end{aligned}
$$

(2.58)

So, it is natural to choose

$$E^{acc}(y) = \sum_{b\in\mathcal{B}}(a_b(y)+c_b(y))$$

as an approximation of $E^a(y)$, because

$$
\begin{aligned}
DE^{acc}(Bx;v) &= \sum_{b\in\mathcal{B}}(Da_b(y)+Dc_b(y)) \\
&\overset{(2.57)}{=} \frac{1}{\varepsilon}\sum_{b\in\mathcal{B}} De_b(Bx;v) \\
&\overset{(2.50)}{=} \frac{1}{\varepsilon}DE^a(Bx;v) \qquad (2.59)
\end{aligned}
$$

2.7 The QCF Method

2.7.1 Strong Formulation

The present section presents a force-based method, the QCF method, the underlying principle behind the most commonly used quasicontinuum software. The concept is the same as that of the *Quasicontinuum Non-Local (QNL)* method, which was the first energy-based model without ghost-forces [22]. In short, the interfacial atoms interact with the atomistic region using the atomistic model and with the continuum region using the continuum model. The first version of QNL was restricted to $R = 2$, but extensions to arbitrary finite range exist [1, 23]. The QCF Method is a force-based coupling method that doesn't present interfacial errors and approximates forces rather than energy, as it does not give a conservative force field. In other words, the equilibrium solutions do not come from minimization of an energy functional [13]. Its formulation starts from the QCL method mentioned above (eqn. 2.42) and the effective atomistic forces F^a given by

$$F^a_m = -\frac{1}{H_m}\frac{\partial E^a(y_h)}{\partial Y_m} \qquad m\in\mathbb{Z} \qquad (2.60)$$

It is essential that F_m^a are defined on the grid X_m and for atoms "well inside" the atomistic area they coincide with the internal atomic forces $f_{i_m}^a$ defined in (2.20). The term "well inside", needs to be clarified : this property holds in particular for the indexes i_m which satisfy $\{i_m - 1, i_m, i_m + 1\} \subset \mathcal{L}_{rep}$. In other words, when three consecutive repatoms are consecutive in the atomistic grid as well.

Proof. In case all three $x_{i_m-1}, x_{i_m}, x_{i_m+1}$ are chosen as repatoms, we have the following image.

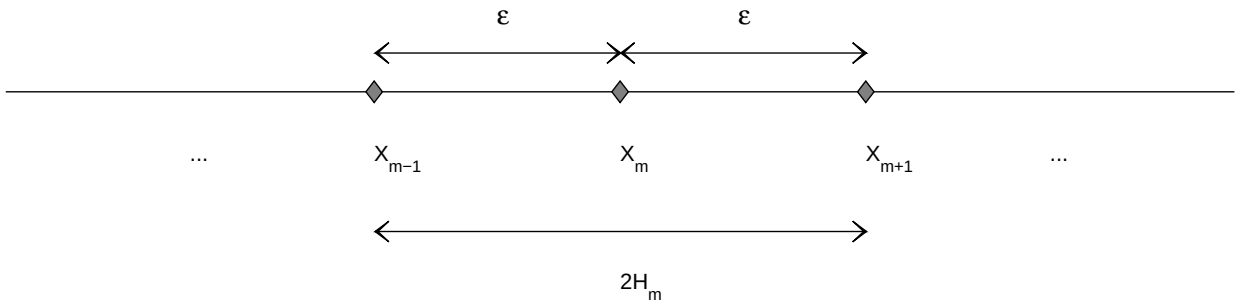

FIGURE 2.7: Three consecutive repatoms.

It is clear that $H_m = \varepsilon$, so:

$$\begin{aligned} F_m^a(y_h) &= -\frac{1}{H_m}\frac{\partial E^a(y_h)}{\partial Y_m} \\ &= -\frac{1}{\varepsilon}\sum_{j\in\mathcal{L}}\frac{\partial E^a(y_h)}{\partial y_j}\frac{\partial y_{h,j}}{\partial Y_m} \\ &\overset{(2.20)}{=} \sum_{j\in\mathcal{L}} f_j^a(y_h) \\ &= f_{i_m}^a(y_h) \end{aligned} \tag{2.61}$$

because

$$\frac{\partial y_{h,j}}{\partial Y_m} = \delta_{j,i_m}$$

■

This remark is effectively used for the atoms in $\mathcal{L}_a$, as, due to the assumption that

$$\{-\kappa - R, \cdots, \kappa + R\} \subset \mathcal{L}_{rep}$$

we will surely have that $F^a_m(y_h) = f^a_{i_m}(y_h)$, $\forall i_m \in \mathcal{L}_a$, so we can define the QCF force operator F^{qcf} for $y_h \in \mathcal{Y}^+_h$ as

$$F^{\text{qcf}}_m(y_h) = \begin{cases} F^a_m(y_h) & i_m \in \mathcal{L}_a \\ \\ F^c_m(y_h) & i_m \in \mathcal{L}_c \end{cases} \tag{2.62}$$

extended periodically. Similarly to the formulation of the atomistic model (2.21) and the QCL method (2.42), we produce the variational problem:

$$\text{find } y^{qc}_h \in \mathcal{Y}^+_h \text{ so that} \quad \left(F^{\text{qcf}}(y^{qc}_h) + g, v_h\right)_h = 0 \qquad \forall v_h \in \mathcal{U}_h \tag{2.63}$$

This is done by breaking the inner product in two, using the ε-inner product (2.6) for the atomistic atoms and maintaining the h-inner product (2.34) for the continuum region. The nonlinear problem (2.63) is the strong formulation of the QCF method. The QCF model doesn't suffer from ghost forces, as one can easily see that it satisfies exactly the conditions (2.21), (2.42) in the respective areas. We see that by talking in terms of forces rather than of energy contributions, we get rid of ghost forces; however, the QCF method has some stability issues [4, 16, 17], attributed to some terms it presents when written in weak form.

2.7.2 Weak Formulation

In this subsection, we will make use of the stress functions. This will allow us to reduce (2.63) to a model that involves only nearest neighbor interactions. We will assume zero external forces $g = 0$; to be included again, they are just added to $F^c_m(y_h)$. Recall from the computation in (2.44), that the variation of $E^{c,h}$ for $y_h \in \mathcal{Y}^+_h$ is

$$\begin{aligned} DE^{c,h}(y_h; v_h) &= \sum_{m=1}^{M} h_m W'(Y'_m) \cdot V'_m \\ &= \sum_{m=1}^{M} h_m \sigma^c_m(y_h) V'_m \qquad \forall v_h \in \mathcal{U}_h \end{aligned} \tag{2.64}$$

where we have defined the *stress functions*

$$\sigma^c_m(y_h) := W'(Y'_m) \tag{2.65}$$

$$= \sum_{r=1}^{R} r\phi'(rY'_m) \tag{2.66}$$

The stresses are related to the forces of the QCL model according to the formula

$$F_m^c(y_h) = \frac{1}{H_m}\left[\sigma_{m+1}^c(y_h) - \sigma_m^c(y_h)\right] \tag{2.67}$$

Proof of (2.67). Indeed,

$$\begin{aligned}\frac{1}{H_m}\left[\sigma_{m+1}^c(y_h) - \sigma_m^c(y_h)\right] &\overset{(2.65)}{=} \frac{1}{H_m}\left[W'(Y'_{m+1}) - W'(Y'_m)\right] \\ &\overset{(2.43)}{=} -\frac{1}{H_m}\frac{\partial E^{c,h}(y_h)}{\partial Y_m} \\ &\overset{(2.41)}{=} F_m^c(y_h)\end{aligned}$$

■

We have mined the stresses with the aim to include only nearest neighbor interactions of the test functions v_h, i.e. the terms V'_m in (2.64). Next, we derive a similar result for the atomistic model from the initial formulation (2.10). We begin with an expression of long-range interactions through "closest-neighbor" ones : for $v \in \mathcal{U}$, $r \in \{1, \cdots, R\}$,

$$\begin{aligned}D_r v_j &= \frac{v_{j+r} - v_j}{r\varepsilon} \\ &= \frac{1}{r\varepsilon}\cdot\left[v_{j+r} - v_{j+r-1} + v_{j+r-1} - \cdots - v_{j+1} + v_{j+1} - v_j\right] \\ &= \frac{1}{r}\cdot\left[\frac{v_{j+r} - v_{j+r-1}}{\varepsilon} + \cdots + \frac{v_{j+1} - v_j}{\varepsilon}\right] \\ &= \frac{1}{r}\cdot\left[v'_{j+r} + \cdots + v'(j+1)\right] \\ &= \frac{1}{r}\sum_{i=j+1}^{j+r} v'_i\end{aligned} \tag{2.68}$$

$$\begin{aligned}(2.10) \Rightarrow DE^a(y;v) &= \varepsilon\sum_{r=1}^{R}\sum_{j=-N+1}^{N}\phi'(rD_r y_j)\cdot rD_r v_j \\ &\overset{(2.68)}{=} \varepsilon\sum_{r=1}^{R}\sum_{j=-N+1}^{N}\sum_{i=j+1}^{j+r}\phi'(rD_r y_j)\cdot v'_i \\ &= \varepsilon\sum_{i=-N+1}^{N}\sum_{r=1}^{R}\sum_{j=i-r}^{i-1}\phi'(rD_r y_j)\cdot v'_i\end{aligned} \tag{2.69}$$

So, the appropriate stresses are

$$\sigma_i^a(y) := \sum_{r=1}^{R}\sum_{j=i-r}^{i-1}\phi'(rD_r y_j) \tag{2.70}$$

and

$$DE^a(y;v) = \varepsilon \sum_{i=-N+1}^{N} \sigma_i^a(y) \cdot v_i' \tag{2.71}$$

The atomic stresses and the internal atomic forces defined in (2.20) are related by

$$f_i^a(y) = \frac{1}{\varepsilon}\left[\sigma_{i+1}^a(y) - \sigma_i^a(y)\right] \tag{2.72}$$

Proof. Indeed,

$$\begin{aligned}
\frac{1}{\varepsilon}\left[\sigma_{i+1}^a(y) - \sigma_i^a(y)\right] &\overset{(2.70)}{=} \frac{1}{\varepsilon}\sum_{r=1}^{R}\left[\sum_{j=i+1-r}^{i}\phi'(rD_r y_j) - \sum_{j=i-r}^{i-1}\phi'(rD_r y_j)\right] \\
&= \frac{1}{\varepsilon}\sum_{r=1}^{R}\left[\phi'(rD_r y_i) - \phi'(rD_r y_{i-r})\right] \\
&= \frac{1}{\varepsilon}\sum_{r=1}^{R}\left[\phi'\left(\frac{y_{i+r}-y_i}{\varepsilon}\right) - \phi'\left(\frac{y_i - y_{i-r}}{\varepsilon}\right)\right] \\
&\overset{(2.22)}{=} -\frac{1}{\varepsilon}\frac{\partial E^a(y)}{\partial y_i} \\
&\overset{(2.20)}{=} f_i^a(y)
\end{aligned}$$

■

We start from the strong formulation (2.63) for $y_h \in \mathcal{Y}_h^+$: (the argument y_h is omitted from all the stresses)

$$\begin{aligned}
\left(F^{\text{qcf}}(y_h), v_h\right)_h &= \sum_{m=1}^{M} H_m F_m^{qc}(y_h)\cdot V_m \\
&= \sum_{i_m \in \mathcal{L}_a} H_m F_m^{qc}(y_h)\cdot V_m + \sum_{i_m \in \mathcal{L}_c} H_m F_m^{qc}(y_h)\cdot V_m \\
&= \sum_{i=-\kappa}^{\kappa} \varepsilon f_i^a(y_h)\cdot v_i + \sum_{m=U+1}^{L-1+M} H_m F_m^{qc}(y_h)\cdot V_m \\
&\overset{(2.72),(2.67)}{=} \sum_{i=-\kappa}^{\kappa}\left[\sigma_{i+1}^a - \sigma_i^a\right]\cdot v_i + \sum_{m=U+1}^{L-1+M}\left[\sigma_{m+1}^c - \sigma_m^c\right]\cdot V_m \\
&= I_1 + I_2
\end{aligned} \tag{2.73}$$

The terms I_1 and I_2 are computed separately:

$$
\begin{aligned}
I_1 &= \sum_{i=-\kappa}^{\kappa} \left[\sigma_{i+1}^a - \sigma_i^a\right] \cdot v_i \\
&= \sum_{i=-\kappa}^{\kappa} \sigma_{i+1}^a \cdot v_i - \sum_{i=-\kappa}^{\kappa} \sigma_i^a \cdot v_i \\
&= \sum_{i=-\kappa+1}^{\kappa+1} \sigma_i^a \cdot v_{i-1} - \sum_{i=-\kappa}^{\kappa} \sigma_i^a \cdot v_i \\
&= \sum_{i=-\kappa}^{\kappa+1} \sigma_i^a \cdot (v_{i-1} - v_i) + \sigma_{\kappa+1}^a \cdot v_{\kappa+1} - \sigma_{-\kappa}^a \cdot v_{-\kappa-1} \\
&= -\sum_{i=-\kappa}^{\kappa+1} \varepsilon \sigma_i^a \cdot v_i' + \sigma_{\kappa+1}^a \cdot v_{\kappa+1} - \sigma_{-\kappa}^a \cdot v_{-\kappa-1}
\end{aligned}
$$

$$
\begin{aligned}
I_2 &= \sum_{m=U+1}^{L-1+M} \left[\sigma_{m+1}^c - \sigma_m^c\right] \cdot V_m \\
&= \sum_{m=U+1}^{L-1+M} \sigma_{m+1}^c \cdot V_m - \sum_{m=U+1}^{L-1+M} \sigma_m^c \cdot V_m \\
&= \sum_{m=U+2}^{L+M} \sigma_m^c \cdot V_{m-1} - \sum_{m=U+1}^{L-1+M} \sigma_m^c \cdot V_m \\
&= \sum_{m=U+2}^{L-1+M} \sigma_m^c \cdot (V_{m-1} - V_m) + \sigma_{L+M}^c \cdot V_{L-1+M} - \sigma_{U+1}^c \cdot V_{U+1} \\
&= -\sum_{m=U+2}^{L-1+M} h_m \sigma_m^c \cdot V_m' + \sigma_L^c \cdot V_{L-1} - \sigma_{U+1}^c \cdot V_{U+1}
\end{aligned}
$$

Now, we divide the domain of the problem, not according to reference points of atoms but based on intervals of the form $I_m = (X_{m-1}, X_m)$ to $\mathcal{M}_a$ and $\mathcal{M}_c$ such that $\mathcal{M}_a \uplus \mathcal{M}_c = \{1, \cdots, M\}$. In the atomistic region we will include all the finite elements with at least one edge in $\mathcal{L}$. So,

$$\mathcal{M}_a := \{L, \cdots, U+1\} \tag{2.74}$$

$$\mathcal{M}_c := \{1, \cdots, L-1\} \cup \{U+2, \cdots, M\} \tag{2.75}$$

Using this notation and the convention that we will be using the repatom numbering everywhere and $\sigma_m^a = \sigma_{i_m}^a$, we complete the calculation of

$$\begin{aligned}\left(F^{\mathrm{qcf}}(y_h),v_h\right)_h &= I_1+I_2\\ &= -\sum_{m\in\mathcal{M}_a}\varepsilon\sigma_m^a\cdot V_m'+\sigma_{U+1}^a\cdot V_{U+1}-\sigma_L^a\cdot V_{L-1}-\\ &\quad -\sum_{m\in\mathcal{M}_c}h_m\sigma_m^c\cdot V_m'+\sigma_L^c\cdot V_{L-1}-\sigma_{U+1}^c\cdot V_{U+1}\end{aligned}$$

$$\begin{aligned}\Rightarrow -\left(F^{\mathrm{qcf}}(y_h),v_h\right)_h = &\sum_{m\in\mathcal{M}_a}\varepsilon\sigma_m^a\cdot V_m'+\sum_{m\in\mathcal{M}_c}h_m\sigma_m^c\cdot V_m'+\\ &-(\sigma_L^c-\sigma_L^a)\cdot V_{L-1}+(\sigma_{U+1}^c-\sigma_{U+1}^a)\cdot V_{U+1}\end{aligned}\tag{2.76}$$

It is easy to see that the extra interfacial terms are unwanted. Indeed, (2.63) implies that

$$\begin{aligned}0 = &-\sum_{m\in\mathcal{M}_a}\varepsilon\sigma_m^a\cdot V_m'-\sum_{m\in\mathcal{M}_c}h_m\sigma_m^c\cdot V_m'+\\ &+(\sigma_L^c-\sigma_L^a)\cdot V_{L-1}-(\sigma_{U+1}^c-\sigma_{U+1}^a)\cdot V_{U+1}\\ \overset{(2.71),(2.64)}{=} &-DE^a(y_h^a;v_h)-DE^{c,h}(y_h^c;v_h)+(\sigma_L^c-\sigma_L^a)\cdot V_{L-1}-(\sigma_{U+1}^c-\sigma_{U+1}^a)\cdot V_{U+1}\\ \overset{(2.19),(2.40)}{=} &(\sigma_L^c-\sigma_L^a)\cdot V_{L-1}-(\sigma_{U+1}^c-\sigma_{U+1}^a)\cdot V_{U+1}\end{aligned}\tag{2.77}$$

These terms affect the stability of the method and are used to derive results regarding consistency and a priori errors, as in [4]. A study for a linearization of the problem was made in [10]. Specifically, the linearized QCF operator has been proven to be non-positive definite and uniform stability cannot be achieved with respect to any norm ([11]). The lack of positive-definiteness complicates a generalization to more dimensions.

2.8 The SAC Method

After the remarks at the end of the previous section, it is natural to introduce a method with the required property. The idea is to do the coupling, not on the level of forces but on the level of stresses. To this end, rewrite equations (2.71) and (2.64).

$$\begin{aligned}&DE^a:\mathcal{Y}^+\to\mathcal{U}^*\\ &DE^a(y;v)=\sum_{i=-N+1}^{N}\varepsilon\sigma_i^a v_i'\end{aligned}\quad\Bigg\|\quad\begin{aligned}&DE^c:\mathcal{Y}_h^+\to\mathcal{U}_h^*\\ &DE^c(y_h;v_h)=\sum_{m=1}^{M}h_m\sigma_m^cV_m'\end{aligned}$$

So, the coupling will give

$$S^{ac} : \mathcal{Y}_h^+ \to \mathcal{U}_h^*$$
$$S^{ac}(y_h; v_h) = \sum_{m \in \mathcal{M}_a} \varepsilon \sigma_m^a \cdot V_m' + \sum_{m \in \mathcal{M}_c} h_m \sigma_m^c \cdot V_m'$$

Using (2.76),

$$S^{ac}(y_h; v_h) = -\left(F^{\mathrm{qcf}}(y_h), v_h\right)_h + (\sigma_L^c - \sigma_L^a) \cdot V_{L-1} - (\sigma_{U+1}^c - \sigma_{U+1}^a) \cdot V_{U+1}$$
$$\overset{(2.77)}{=} (g, v_h)_h$$

So, we impose weakly that the stresses are equal at the interface and end up to the stress-based atomistic/continuum (SAC) method

$$\text{find } y_h^{ac} \in \mathcal{Y}_h^+ \text{ so that} \quad S^{ac}(y_h^{ac}; v_h) = (g, v_h)_h \qquad \forall v_h \in \mathcal{U}_h \tag{2.78}$$

This method was first suggested and studied in [3, 4]. In short, the SAC approximation is valid whenever the atomistic solution is stable and the linearized S^{ac} operator *is* positive definite. It is still tricky though, to write down an SAC method in 2-D or 3-D, since stress functions are not uniquely defined.

3 Numerical results

All numerical simulations ran in MATLAB, using the Optimization Toolbox. For the energy-based methods, as well as for the atomistic (accurate) model, we used the `fminsearch` function, which finds the local minimum of a real-valued scalar function of several variables, starting at an initial estimate. To be sure that this local minimum is the equilibrium solution we look for, the initial estimate is the solution of the atomistic model and we set the options: `MaxIter` to 2000, `TolFun` and `TolX` to 1.e-12. The atomistic approximation itself was obtained with even stricter tolerance options. For the energy-based methods see Section 3.1. The QCF and SAC methods were implemented using the algorithm described in [15] (see Section 3.2). More details of the simulations are below.

3.1 Some words about optimization

For the problem of unconstrained minimization of a general non-linear function, one can choose from an arsenal of numerical methods to approximate a point of minimum. Most iterative methods converge to a point of local minimum which under certain conditions is also a global minimum. Some methods are applied especially on functions with specific characteristics while others have broader scope. The problem of minimization belongs to a larger area of numerical mathematics : optimization. In 1960s, a variety of methods emerged, methods that are used today, either in their initial forms or after modifications and improvements. All these techniques can be grouped in three categories based on the main idea : the conjugate direction methods, second derivative methods and direct search methods [24, 25, 29]. I will make a brief description of each and elaborate on the Nelder-Mead algorithm, the direct search method which I used for my computations.

3.1.1 Conjugate direction methods

When the Hessian matrix of the objective function is not available or difficult to compute, one can use a conjugate gradient method. In general, these are iterative methods that perform a line-search at every iteration in a direction decided on-the-spot. The term ”conjugate” refers to the set of candidate directions that need to be mutually independent. Smith, Fletcher, Powell, Zangwill and Rhead have all worked on a conjugate direction method using no derivatives.

However, even with all the improvements, its convergence is slow for general functions and $n > 10$, so it is preferable to use the *conjugate gradient method* which chooses the steepest descent direction subject to conjugacy conditions and requires the function's gradient. Other methods are Powell's method, which reduces iteratively the dimension of the search space, and Partan method, which executes a steepest descent step and a line search to that direction.

3.1.2 Second derivative methods

If the Hessian matrix of the objective function is known (or easily approximated), second derivative methods offer reliability and fast convergence. Typical examples are the *Newton's method* and its variants. Again, a line search is made but this time the Hessian matrix is employed. Variants are *Greenstadt's method*, *Marquardt-Levengberg method* and *Quasi-Newton methods*.

3.1.3 Direct search methods

Methods that fall into this category produce a sequence of approximations by comparing values of the objective function only, making no use of its gradient or any approximation to it. Thus, they are useful in case the function is non-differentiable, has discontinuous first-order derivatives or the computation of the gradient is complex. Elementary examples of direct search methods are the *bounded methods*. A notable bounded method is the generalized Fibonacci search that, based on the Fibonacci numbers, narrows down the interval containing the optimum point. Another popular strategy is to pick a destination (or destinations) and minimize along it. In its simplest form, this is the *alternating variable method* (or *compass search*), which minimizes with respect to every co-ordinate one at a time periodically until termination conditions are satisfied. This can work for specific cases but in general slow (or even none at all) convergence is observed. This is mainly due to the fact that the directions are fixed throughout the process; in 1961 Hooke and Jeeves suggeseted the *pattern search method* that includes "exploring" around the current point and move accordingly to the suitable direction. Variants of the Hooke and Jeeves method are the *Spider method* and *razor search*. A similar concept is behind *Rosenbrock's method*, but a whole new orthonormal set of directions is generated in every iteration while expanding, contracting and reversing exploration steps. Finally, there is the *simplex method* which uses regular simplexes of $\mathbb{R}^n$ reflecting the "worst" vertex with respect to the centroid of the rest of the vertices at every iteration. This way the simplex moves towards smaller values of the objective function.

The method that I used for the implementation of the methods described in Chapter 2 is the *Nelder-Mead simplex method*, an improved version of the classic simplex method. Nelder and Mead decided to rescale the simplex depending on the result of the reflection. As all my numerical results were taken using this algorithm, it is presented below. I include the algorithm and a presentation of all possible cases for $\mathbb{R}^3$.

In words, the algorithm is described as substituting the "worst" vertex of the current simplex with a "better" point. Of course, these labels are based on the values of the objective function on the current simplex vertices. During this process, the simplex becomes expanded or contracted depending on the specific points selected by reflection. Starting with an initial simplex of $n+1$ points not lying on a hyperplane $\{\vec{x}_k\}_{k=1}^{N+1}$, the algorithm points out the vertices (out of all $N+1$ that define the simplex) that give the best, the worst and the second-worst value to f;as this is a minimization

problem, this criterion is reduced to determining w, s, b indices s.t.

$$f(x_w) = \max_{1\le k\le N+1} f(x_k), \quad f(x_s) = \max_{\substack{1\le k\le N+1 \\ k\neq w}} f(x_k), \quad f(x_b) = \min_{1\le k\le N+1} f(x_k) \tag{3.1}$$

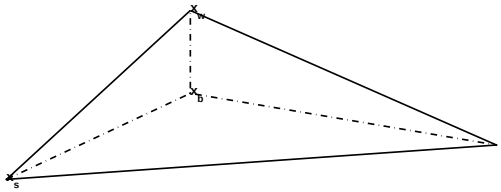

FIGURE 3.1: Initial simplex

Every iteration of the method changes the simplex by using only the function values on specific points. The first approach is to substitute the worst point with a better one. The first candidate is the reflection x_r of x_w with respect to the centroid of the rest of the vertices, called

$$x_0 = \frac{1}{N} \sum_{\substack{i=1 \\ i\neq w}}^{N+1} x_i \tag{3.2}$$

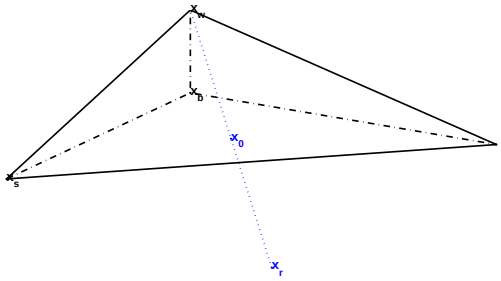

FIGURE 3.2: Reflection

If this point is better than x_w but still worse than x_b, it replaces x_w.

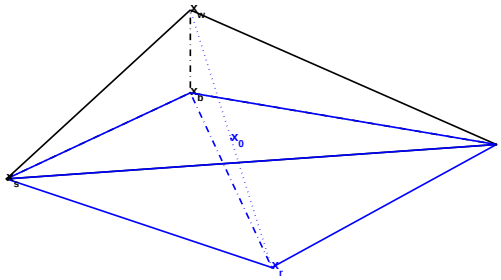

FIGURE 3.3: Reflection successful. The new simplex is the blue one.

If it is better than our best x_b, we attempt an expansion towards its direction with the hope of getting an even better point x_e.

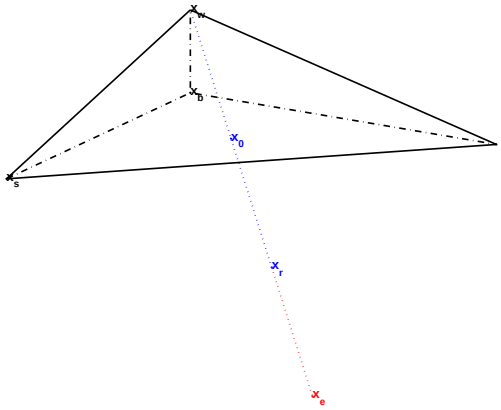

FIGURE 3.4: Expansion

x_w is replaced either by x_r

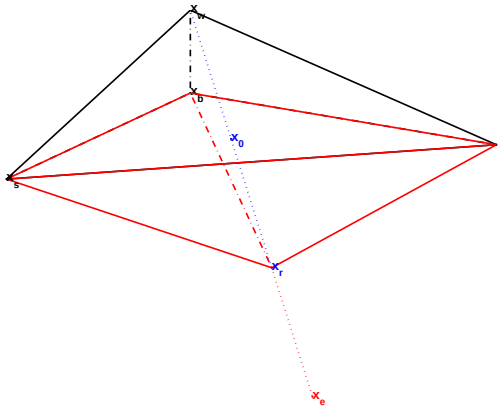

FIGURE 3.5: Expansion unsuccessful; the new simplex is the red one, where x_r replaces x_w

or by x_e (whichever suits us better).

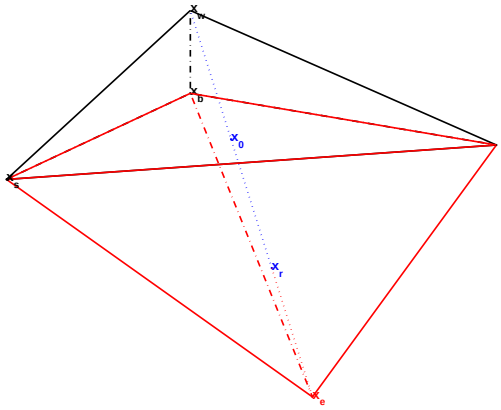

FIGURE 3.6: Expansion successful; the new simplex is the red one, where x_e replaces x_w

In case x_r is worse than the worst point, we try a contraction.

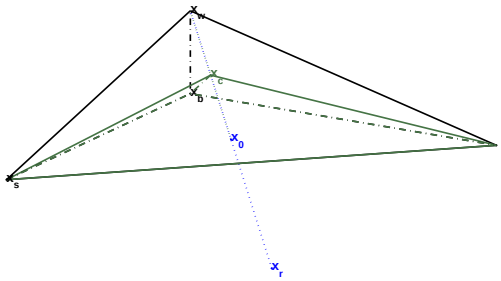

FIGURE 3.7: If $f(x_c) < f(x_w)$, substitute x_w by x_c

If this doesn't work either, we shrink the initial simplex and start over.

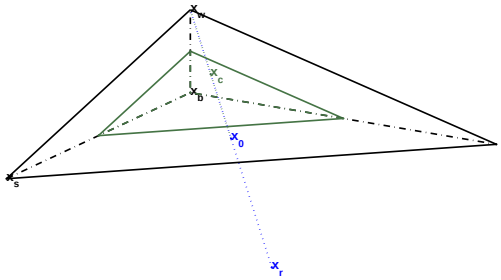

FIGURE 3.8: Start over with a shrunken simplex.

The geometrical operations of reflection, expansion, contraction and shrinkage are determined by the parameters $\alpha, \gamma, \rho, \sigma$ respectively. For our implementation the values are $1, 2, {}^1/_2, {}^1/_2$. The procedure continues until some criteria of tolerance are satisfied (usually in the form of ε-small standard deviation of $\{f(x_k)\}_{k=1}^{N+1}$) or until a maximum number of iterations has been exhausted.

Algorithm 1 Nelder-Mead method($f, \{\vec{x}_k\}, \alpha, \gamma, \rho, \sigma$, tol, MaxIter)

$i \leftarrow 0$
while $i < MaxIter$ && stdev$(f(x_k)) > tol$ **do**
  find w, s, b indices s.t. (3.1) holds
  calculate x_0 using (3.2)
  find the reflection of the worst vertex wrt to x_0 as $x_r = (1+\alpha)x_0 - \alpha x_w$
  if $f(x_b) \leq f(x_r) < f(x_s)$ **then**
    $x_w \leftarrow x_r$
  else if $f(x_r) < f(x_b)$ **then**
    compute $x_e = (1+\gamma)x_0 - \gamma x_w$
    if $f(x_e) < f(x_r)$ **then**
      $x_w \leftarrow x_e$
    else
      $x_w \leftarrow x_r$
    end if
  else
    compute $x_c = (1-\rho)x_w + \rho x_0$
    if $f(x_c) < f(x_w)$ **then**
      $x_w \leftarrow x_c$
    else
      for $k = 1$ **to** $N+1, k \neq b$ **do**
        $x_k \leftarrow (1-\sigma)x_b + \sigma x_k$
      end for
    end if
  end if
  $i \leftarrow i+1$
end while

At this point, I would like to explain the choice of algorithm : direct search methods are an effective option (and sometimes the only one) for several optimization problems. One could argue that they are not strictly supported mathematically and they are based on heuristics [21]. This is exactly the reason why I implemented most of the methods using the Newton's method, but for the energy functions of some of the QC methods the condition number of the Hessian matrix or its approximation would become very large. However, for the methods I got final results they were almost identical to the ones given by the Nelder-Mead algorithm, so, for reasons of uniformity, I chose to use N.M. on all of them.

3.2 Ghost force correction algorithm

To solve the equilibrium equation of the strong form of the QCF method (2.63), we implemented the algorithm described in [15]. The same algorithm or slightly different definitions of it have also been used in [13, 12, 16, 17]. We have already explained the reason behind the existence of ghost- forces. The concept of this technique is to balance the forces in the areas of the discrepancy. Each representative atom has forces acting on it as though it were surrounded by representative atoms of the same type.
Define for a deformation $y_h \in \mathcal{Y}_h^+$

$$(\mathrm{gfc}(y_h))_m := F_m^{qcf}(y_h) - f_{i_m}^a(y_h) \tag{3.3}$$

Because of the definition of F^{qcf} and the remark 2.61, for our model

$$(\mathrm{gfc}(y_h))_m = 0 \qquad m = L, \cdots, U$$

Then this correction is normally applied during a quasistatic loading process.

Algorithm 2 Ghost Force Correction$(y_0, \delta B)$

1: **for** $k = 1, \cdots$ **do**
2: $\quad y_n \leftarrow \arg\min \{E^{qce}(y) - (g,y)_\varepsilon - (\mathrm{gfc}(y_{n-1} + x\delta B), y)_h\}$
3: **end for**

As initial approximation, we inserted the atomistic solution and $\delta B = 0.01$;the number of iterations is determined by tolerance criteria. In practise, for all the runs we include not more than ten iterations were necessary. The same iterative algorithm was used for the SAC method and the suitable force function.

3.3 Results

This 1-D problem involves many parameters, each of which can be studied separately in order to make a verdict on its role. The codes we have available in MATLAB can be used to simulate many possible sets of data. Here, a specific input is presented : $N = 1000,\ R = 2,\ B = 1,\ \kappa = 3,\ CG = 32$ and

Test 1 zero external forces

$$g_i = 0 \qquad \forall i \in \mathcal{L}$$

Test2 crack at the origin

$$g_i = \begin{cases} -1 - x_i, & i = -N+1, \cdots, -2 \\ -{}^{N}/_{4}, & i = -1 \\ {}^{N}/_{2}, & i = 0 \\ -{}^{N}/_{4}, & i = 1 \\ 2 - x_i, & i = 1, \cdots, N \end{cases} \tag{3.4}$$

The parameter CG is used to determine the level of coarse-graining : repatoms in Ω_c are chosen to be the points of a uniform grid with step $CG \cdot \varepsilon$. The external dead loads gathered in g are intentionally picked, so that the exact (atomistic) solution simulates a crack at the origin. All errors are computed in the $\mathcal{U}^{1,\infty}$-norm (2.5). Also, for the plots the x-axis has been scaled to $[0,1]$. The methods are grouped as follows : QCE, ECC and ACC, QCF and SAC; this is done, because the $\mathcal{U}^{1,\infty}$-distance between y^{ECC} and y^{ACC} (or y^{QCF} and y^{SAC}) is $O(10^{-6})$. As mentioned in Section 2.4, the QCE method presents errors near the interface, whereas ECC, ACC, QCF and SAC achieve high accuracy in Ω apart from the crack location (second test).

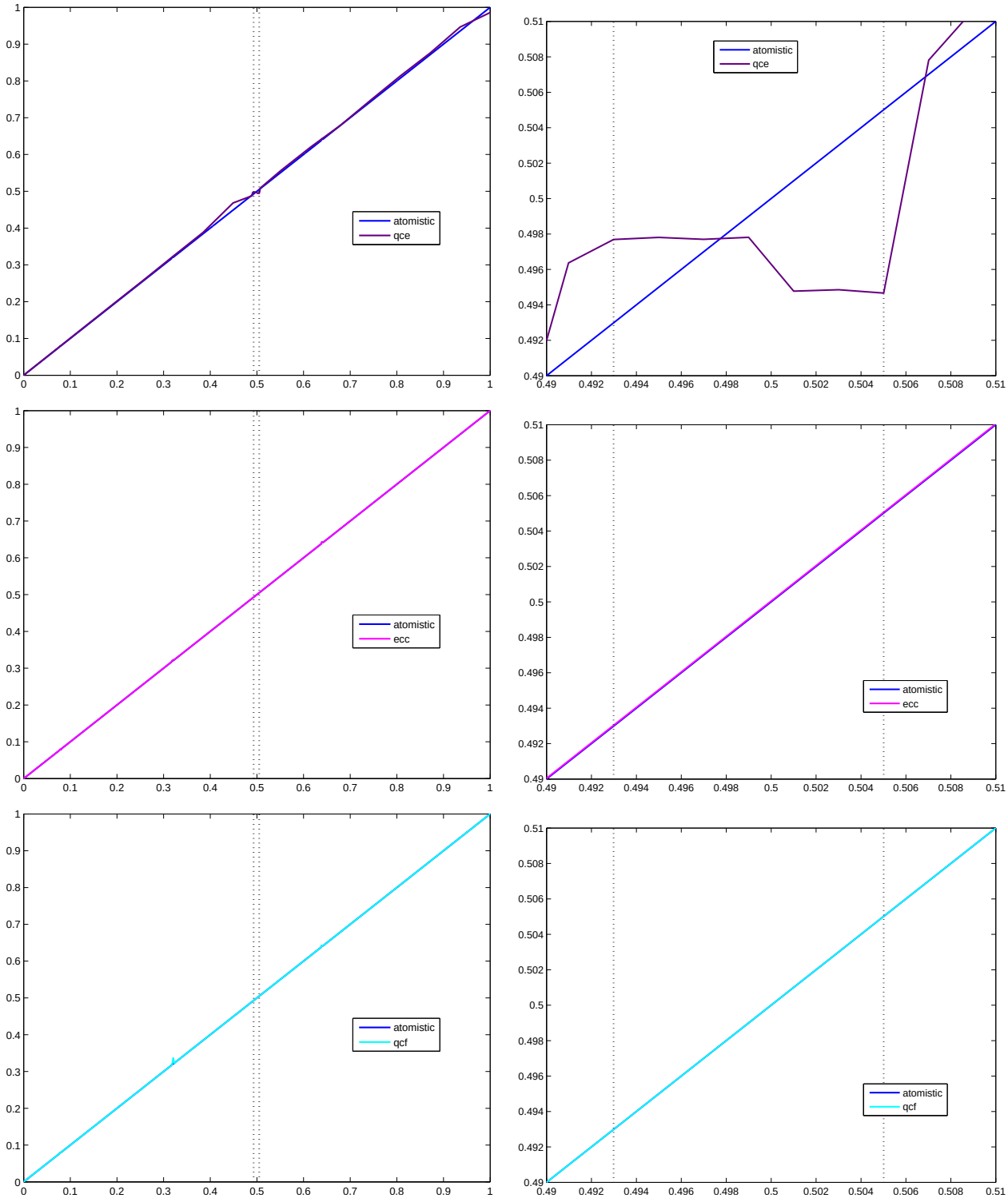

FIGURE 3.9: Test 1 : **left:** the whole domain **right :** a close up including all the atomistic region Ω_a which is between the black dotted lines

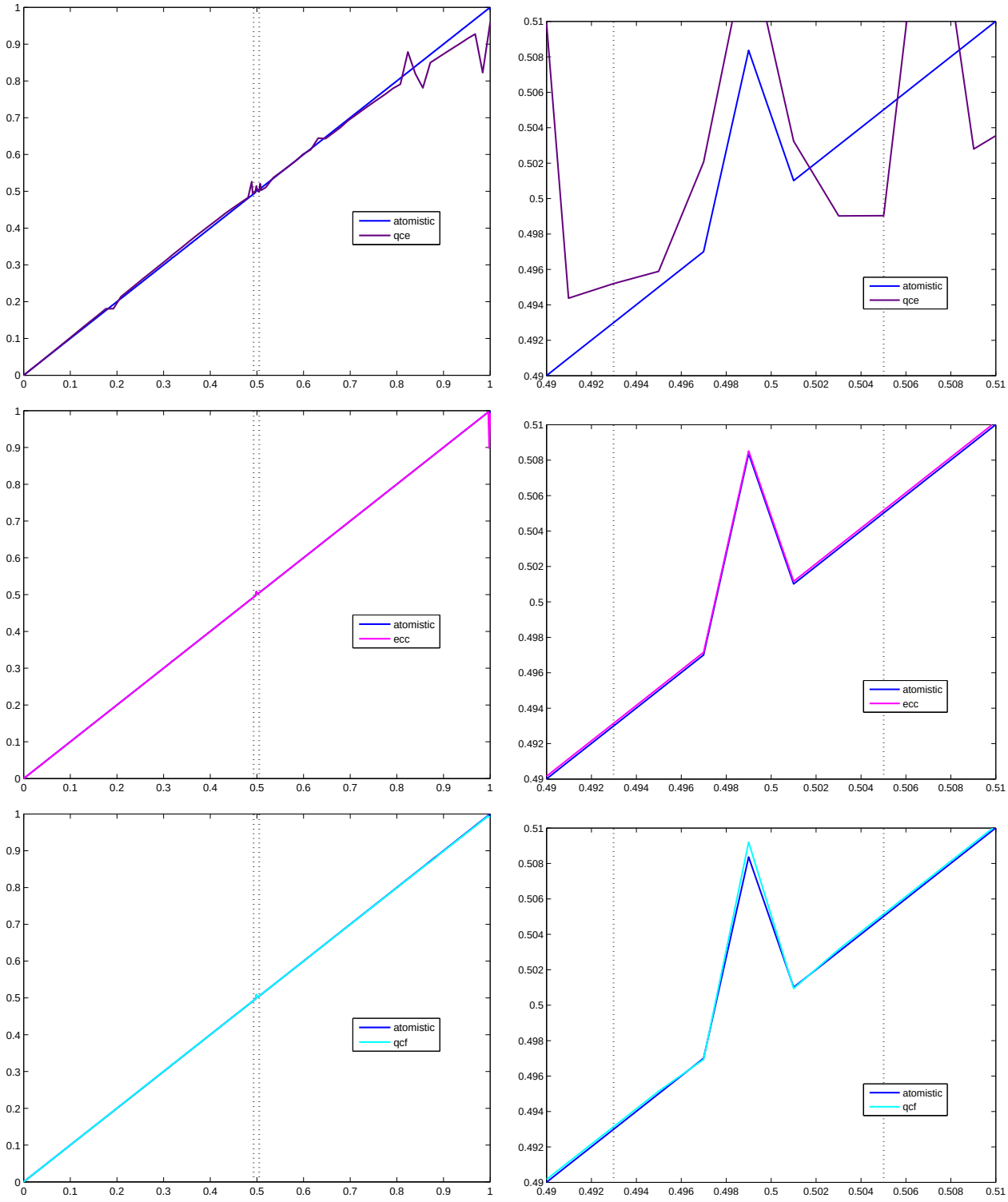

FIGURE 3.10: Test 2 : **left:** the whole domain **right :** a close up including all the atomistic region Ω_a which is between the black dotted lines

The level of coarse-graining against the errors of each method is plotted below. Remember $CG = 1$ means we have the fully atomistic grid and as CG increases the grid is coarsened. The QCE method, due to the problem of ghost

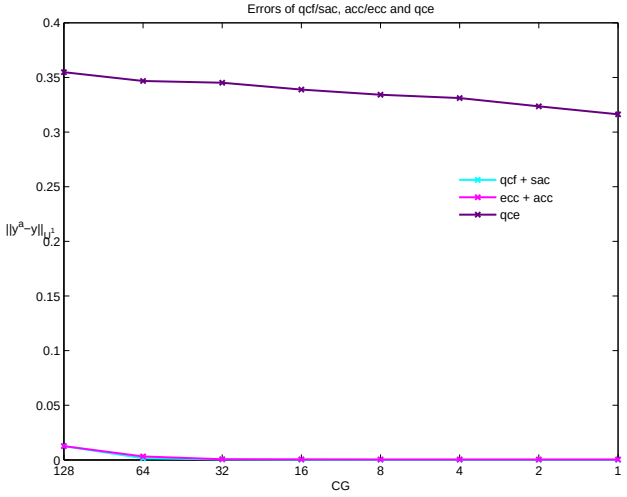

forces, presents significant error. Zooming in only on the other two options The two methods both perform well and,

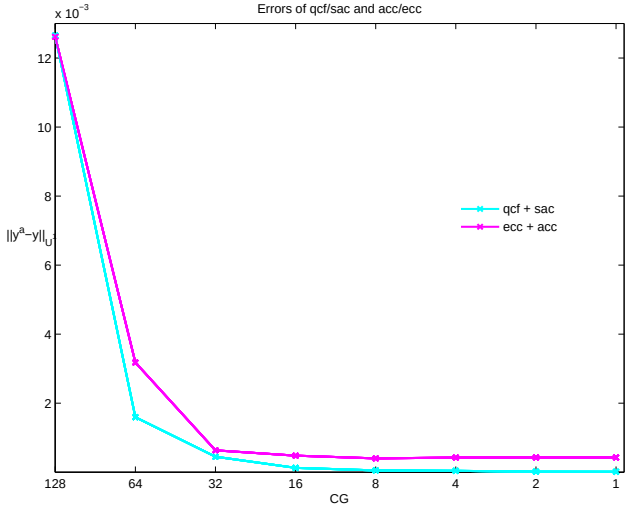

as atomistic accuracy is approached, they seem to end up in a flat line; this is due to the inevitable model error. For values of CG less than 8 the modeling error is more significant than the coarse-graining error [4].

3.4 Possible future projects

There is still a lot left to be examined on QC methods. They appear to be promising thanks to their computational potential and accuracy and have already been modified to meet needs of specific applications [7, 8, 9, 19]. Aspects that could give rise to new directions are : generalization to 2-D or 3-D [1], improved mesh generation, faster solvers of the equilibrium equations, strong theroetical basis for a priori computational results [17], parallelization etc.

Bibliography

[1] A. V. Shapeev, *Consistent energy-based atomistic/continuum coupling for two-body potential: 1D and 2D case*

[2] C. A. Felippa, *Numerical experiments in finite element grid optimization by direct energy search*, Appl. Math. Modelling, Vol 1 (1977)

[3] C. Makridakis, C. Ortner and E. Süli, *Stress-based atomistic/continuum coupling: a new variant of the quasicontinuum approximation*

[4] C. Makridakis, C. Ortner and E. Süli, *A priori error analysis of two force-based atomistic/continuum hybrid models of a periodic chain*

[5] C. Ortner and E. Süli, *Analysis of a quasicontinuum method in one dimension*, ESAIM: M2AN, 42(1):5791 (2008)

[6] E. B. Tadmor, M. Ortiz and R. Phillips, *Quasicontinuum analysis of defects in solids*, Phil Mag A, Vol 73, pp 1529-1563 (1996)

[7] E. B. Tadmor, R. Miller and R. Phillips, *Nanoidentation and incipient plasticity*, J Mater Res, Vol 14, No. 6 (1999)

[8] L. Truskinovsky and A. Vainchtein, *Dynamics of martensitic phase boundaries: discreteness, dissipation and inertia*, Continuum Mech. Thermodyn. 20:97-122 (2008)

[9] L. Truskinovsky and A. Vainchtein, *Kinetics of martensitic phase transitions : lattice model*

[10] M. Dobson, C. Ortner and A. Shapeev, *Stability of the force-based quasicontinuum method*, arXiv:1004.3435 (2010)

[11] M. Dobson, C. Ortner and A. Shapeev, *Stability, instability and error of the force-based quasicontinuum approximation*, arXiv:0903.0610 (2009)

[12] M. Dobson and M. Luskin, *Analysis of a force-based quasicontinuum approximation*, ESAIM: M2AN, 42(1):113-139 (2008)

[13] M. Dobson and M. Luskin, *Iterative solution of the quasicontinuum equilibrium equations with continuation*, J Sci Comput 37: 1941 (2008)

[14] M. Dobson and M. Luskin, *An optimal order error analysis of the one-dimensional quasicontinuum approximation*, SIAM J Numer Anal, 47:2455-2475 (2009)

[15] M. Dobson, M. Luskin and C. Ortner, *Iterative methods for the force-based quasicontinuum approximation*

[16] M. Dobson, M. Luskin and C. Ortner, *Sharp stability estimates for the force-based quasicontinuum method*

[17] M. Dobson, M. Luskin and C. Ortner, *Stability, instability and error of the force-based quasicontinuum approximation*

[18] P. Lin, *Theoretical and numerical analysis for the quasicontinuum approximation of a material particle model*, Mathematics of Computation, Vol 72, No 242, pp 657-675 (2002)

[19] Q. Peng, X. Zhang, L. Hung, E. A. Carter and G. Lu, *Quantum simulation of materials at micron scales and beyond*, Physical Review B 78, 054118 (2008)

[20] R. E. Miller and E.B. Tadmor, *The quasicontinuum method: overview, applications and current directions*, Journal of Computer-Aided Materials Design, 9:203-239 (2002)

[21] T. G. Kolda, R. M. Lewis and V. Torczon, *Optimization by direct search : new perspectives on some classical and modern methods*, SIAM, Vol 45,No 3, pp 385482 (2003)

[22] T. Shimokawa, J. Mortensen, J. Schiotz and K. Jacobsen, *Matching conditions in the quasicontinuum method : removal of the error introduced at the interfacebetween the coarse-grained and fully atomistic region*, Phys Rev B, 69(21):214104 (2004)

[23] X. H. Li and M. Luskin, *A generalized quasi-nonlocal atomistic-to-continuum coupling method with finite range interaction*

[24] A. Quarteroni, R. Sacco and F. Saleri, *Numerical Mathematics*, Springer-Verlag (2000)

[25] D. Kincaid and W. Cheney, *Numerical Analysis : Mathematics of Scientific Computing*, 3rd edition, Brooks/Cole (2002)

[26] H. Brezis, *Functional Analysis : Theory and Applications*, ntua press (1997)

[27] P. G. Ciarlet, *Introduction to Numerical Linear Algebra and Optimization*, Cambridge University Press (1989)

[28] S. C. Brenner and L. R. Scott, *The Mathematical Theory of Finite Element Methods*, 2nd edition, Springer-Verlag (2002)

[29] W. Murray, *Numerical Methods for Unconstrained Optimization*, Academic Press, London and New York (1972)